CrossMark

ORIGINAL PAPER

Accelerated Hot Corrosion Studies of D-Gun-Sprayed Cr_2O_3–50% Al_2O_3 Coating on Boiler Steel and Fe-Based Superalloy

Amita Rani[1] · Niraj Bala[2] · C. M. Gupta[3]

Abstract In the current investigation, Cr_2O_3–50% Al_2O_3 coating was deposited on ASTM-SA213-T-22 boiler steel and Fe-based superalloy Superfer 800H by D-gun spray process. The high-temperature corrosion performance of the coated as well as bare alloys was evaluated in Na_2SO_4–60%V_2O_5 molten salt, an aggressive environment at 900 °C under cyclic conditions. The kinetics of the corrosion were analyzed by the change in weight measurements which were taken after each cycle (i.e., 1-h heating in a tube furnace followed by 20-min cooling in ambient air) for a total period of 50 cycles. The X-ray diffraction and scanning electron microscopy/ energy-dispersive X-ray analysis techniques were used for the analysis of corrosion products. During investigations, it was found that both the selected bare alloys have suffered intensive spallation in the form of removal of their oxide scales, which may be attributed to the formation of non-protective Fe_2O_3-dominated oxide scales, whereas the coated alloys have shown lesser weight gains along with better adhesiveness of the oxide scales with the substrate till the end of the experiment. The oxides of chromium and aluminum were the main phases revealed in the oxide scales of the coated specimens, which are reported to be protective against the hot corrosion.

Keywords Hot corrosion · Detonation gun coating · Superalloys · Cr_2O_3–50% Al_2O_3 coating

✉ Niraj Bala
nirajbala1@rediff.com

1 P.T.U., Jalandhar 144001, India

2 Mechanical Engineering, B.B.S.B.E.C., Fatehgarh Sahib 140407, India

3 Chemistry Department, Government College, Muktsar 1520267, India

Springer

Introduction

The advancements in the development of cooling schemes and high-temperature materials are supposed to increase the life time of boilers and gas turbines with improvements in their properties, i.e., strength, fatigue and creep [1]. A special attention is required as the combination of higher temperature with low-grade fuels and contaminants of working environment such as vanadium, sulfur, sodium and chlorine, demonstrated in the boiler and gas turbine environments, leads to the phenomenon of hot corrosion. Eliaz et al. [2] have defined hot corrosion as accelerated corrosion which is due to the presence of Na_2SO_4-, NaCl-, and V_2O_5-like salt contaminants that combine to form molten deposits, which causes damage to the protective scale by dissolving surface oxides. According to Khanna [3] and Marriott [4], the hot corrosion is the key factor in determining the life of the boiler components. Prakash et al. [5] have conducted a case study of boiler tube failure in coal-fired boilers covering one year, and it was observed that more than 50% of the failures were endorsed to the hot corrosion and erosion due to ash. A very intense corrosive media particularly near the superheater tubes of the boilers is generated by the combustion of coal [6]. These are the major areas where critical high-temperature fireside corrosion problems are encountered. The SO_2 generated due to combustion of sulfur present in coal and fuel oils gets partially oxidized to SO_3. Then, the SO_3 and water vapor react with NaCl (present either as impurities in the fuel or in the air) at combustion temperature to capitulate Na_2SO_4. Small amount of vanadium present in the fuel oils forms V_2O_5 on combustion, thus further reacting with Na_2SO_4 to form sodium vanadate (low melting), which are reported extremely corrosive to the materials used in the combustion system at higher temperatures [2]. The sodium vanadyl vanadate, $Na_2O \cdot V_2O_4 \cdot 5V_2O_5$ is the most common deposit found on boiler superheaters having melting point 550 °C which corrodes metals by long-term contact at a temperature above its melting point [7]. The superalloys have been developed for applications at high temperature, but are not able to meet the requirements of both the high-temperature strength and erosion–corrosion resistance simultaneously [7]. Recent studies showed that the materials used for high-temperature applications are highly prone to hot corrosion and the surface engineering plays a key role in effectively combating the hot corrosion problem [9]. One of the protective means to thwart the problem of hot corrosion is to develop a protective layer (coating) on the base material using various surface modification techniques. The protective coatings are being used extensively nowadays, on structural alloys in energy conversion and consumption systems in order to protect their surface from degradation due to high-temperature oxidation [10]. This is the favored approach, even for the relatively hot corrosion-resistant alloys, which are costly too [11]. As per the literature accessible, the detonation gun (D-gun) spray coating process which is a thermal spray process gives an exceedingly good adhesive strength with low porosity and the coated surface with residual stresses (compressive). Also the porosity values in case of D-gun-sprayed coatings are reported to be very much lower of the order <0.8% than that of the surfaces coated with plasma or HVOF-sprayed techniques [12–15]. The Pratt and Whitney group

initiated a program in the late 1960s, to develop coatings on substrates with compositions which are ostensibly independent of the substrates for a wide range of necessities of gas turbine applications [16, 17]. This means in order to meet the particular environmental service conditions, the chemical composition of an overlie coating can be purposely designed and produced. Coatings are typically designed in such a way that the selective oxidation of an element occurs to form a protective oxide scale such as Cr_2O_3, Al_2O_3 or SiO_2 on revelation to reactive environments [18].

There is no reported literature on hot corrosion behavior of Cr_2O_3–50% Al_2O_3 coating deposited on the selected substrates by detonation gun (D-gun) spray technique. The present work has been focused to study the influence of the Cr_2O_3–50% Al_2O_3 coating developed with D-gun spraying technique, on hot corrosion behavior of ASTM-SA213-T-22 boiler steel and Fe-based superalloys Superfer 800H, in an hostile environment of Na_2SO_4–60%V_2O_5 molten salt at 900 °C under repeated conditions. The selection of the Na_2SO_4–60%V_2O_5 salt hot corrosion environment in the present investigation is due to the reason that it simulates comparable conditions of the deposits of molten sulfate-vanadate, which are ensuing from the condensation of the combustion products of low-grade fuels in boilers [19]. These low melting compounds react and liquefy the protective oxides which are formed on the boiler components. The thermogravimetry technique was employed to investigate the kinetics of the high-temperature corrosion of the selected coating and bare alloy substrates. In order to render an insight into the corrosion mechanisms, the corrosion products were characterized using X-ray diffraction (XRD), scanning electron microscopy/energy-dispersive analysis (SEM/EDAX) and X-ray mapping techniques.

Experimental Procedures

Development of the Coatings

Substrate Material

The Fe-based substrate materials selected for this study are 2.25Cr–1Mo steel "ASTM-SA213-T-22 (Grade T22)" and Fe-based superalloy having Midhani Grade Superfer 800H, in the tube form and rolled sheet form, respectively. The chemical composition of the selected base materials is provided in Table 1, presenting the nominal and actual composition (measured by spectroscopy).

Coating Powder

A commercially available Ni–20Cr (Praxair NI-105) metallic powder was used for developing bond coat, and the Cr_2O_3–50% Al_2O_3 powder for top coat was prepared in laboratory ball mill for 7 h to form a uniform mixture from two types of commercially available alloy powders, namely chromia (Cr_2O_3) with minimum assay 99.5% (AMPERIT® 704 H. C. Starck) and alumina (Al_2O_3) with minimum

Table 1 Chemical composition (wt%) of "ASTM-SA213-T-22 (Grade T-22)" boiler steel and Superfer 800H superalloy

Elements	Alloy grade			
	ASTM-SA213-T-22		Superfer 800H	
	Nominal	Actual	Nominal	Actual
C	0.15	0.15	0.1	0.1
Mn	0.3–0.6	0.45	1.0	1.3
Si	0.5	0.25	0.6	1.0
S	0.03	0.006	–	–
P	0.03	0.03	–	–
Cr	1.9–2.6	2.46	19.5	20
Mo	0.87–1.13	0.80	–	–
Ni	–	–	30.8	32
Ti	–	–	0.44	0.34
Al	–	–	0.34	0.30
Fe	Balance	Balance	Balance	Balance

assay 98.0% (AMPERIT[®] 740; H. C. Starck). The coating powders were made available by SVX Powder M Surface Engineering (Pvt.) Limited, Greater Noida (UP), India. A SEM (scanning electron microscope) micrograph of the selected Cr_2O_3–50% Al_2O_3 powder for top coat is shown in Fig. 1, which represent asymmetrical morphology of the powder particles with larger particle of 41.93 μm size and smaller one of 6.58 μm size as measured by backscattered electron image (BSEI); the results are consistent with the nominal size range provided by the manufacturer.

Coating Formulation

Specimens with dimensions of around 20 mm × 15 mm × 5 mm were cut from the alloy sheets/tubes, polished using SiC papers of 220, 400, 600 grit sizes and
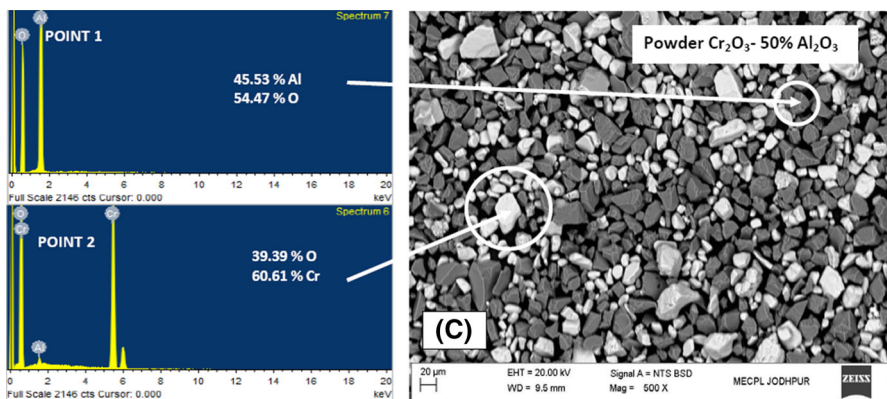
Fig. 1 SEM micrograph of Cr_2O_3–50% Al_2O_3 coating powder

subsequently on 1/0, 2/0, 3/0 and 4/0 grades, and afterward cleaned, degreased and shot-blasted with alumina powders (Grit 60) prior to the deposition of the coatings for developing better adhesion between the substrates and the coatings. The coatings were developed on the substrates using detonation gun (D-gun) spray (a thermal spray process) apparatus. The coating work was carried out by SVX Powder M Surface Engineering Private Limited, Greater Noida (India). The process parameters for the D-gun spray process engaged for developing the coatings are summarized in Table 2.

Characterization of the As-Sprayed Coatings

The coated samples were wheel-polished and then subjected to X-ray diffraction (XRD) analysis and Field Emission Scanning Electron Microscope (FEI Quanta 200F, Made in Czech Republic; at IITR, Roorkee) with EDAX Genesis software attachment and (FEI: CARL ZEISS EVO-18 Research; at Metallizing Equipment Co. PVT. LTD. Jodhpur) fitted with an EDAX attachment (Oxford, UK). This equipment was used to characterize the morphology of the surface as well as cross section along with X-ray mapping of the coatings. SEM micrographs along with EDS spectrum were taken with an electron beam energy of 20 keV. The XRD analysis was performed using a Bruker AXS D-8 Advance diffractometer (Germany) with Cu K radiation source. The specimens were scanned in 2θ range of 20°–120° with a scanning speed of $_2$O/min, and the intensities were recorded. The

Table 2 Process parameters employed during D-gun spray process

Working gases	Fuel gas	Fuel gas	Carrier gas
	Oxygen	Acetylene	Nitrogen
Pressure of working gases (MPa)	0.2	0.14	0.4
Flow rate of working gas (LPH)			
For bond coat (Ni–20Cr)	2800	2240	720
For coating (Cr_2O_3-x Al_2O_3)	4800	1920	1020
Spraying distance (mm)	For bond coat (Ni–20Cr)	For coating (Cr_2O_3–xAl_2O_3)	
	165	180	
Consumption of powder per shot (g/shot)	0.05–0.02		
Water consumption rate (l/mm)	15–25		
Firing rate (Hz)	1–10		
Diameter of accelerating portion of barrel	0.022 m		
Coating thickness per shot (μm)	5–25		
Sound pressure level (dB)	150		
Relative humidity of air (%age)	0.50%		
Coating capacity at the rate of 7 μm/shot (m^2/h)	0.75		
Power supply from mains	Frequency (Hz)	Voltage (volts)	Power (VA)
	50–60	430	450

diffractometer was interfaced with the Bruker DIFFRAC Plus X-ray diffraction software which provides the *d* values directly on the diffraction pattern. To identify the cross-sectional details, the samples were cut with a slow-speed diamond cutter (Buehler's Precision Diamond Saw, Model ISOMET 1000, made in USA) across its cross section, subsequently cold epoxy mounted in plastic rings using cold setting resin (supplied by Kishore Scientific, Delhi) and cold setting hardener (supplied by Kishore Scientific, Delhi) in 1:1 ratio. The mounted samples were subjected to mirror polishing using SiC papers of 220, 400, 600 grit sizes and afterward on 1/0, 2/0, 3/0 and 4/0 grades, successively. Fine polishing was carried out to obtain a mirror finish using a 0.05-μm alumina powder suspension. The polished samples were characterized to obtain their cross-sectional morphology and compositions by using the FE-SEM/EDAX analysis. The EDAX Genesis software was used to calculate the composition of the elements in the coatings from their corresponding emitted X-ray peaks. Cross-sectional microhardness of the coating was measured with Vickers indenter at a load of HV 0.3 kg using microhardness tester (model SHIMADZU HMV-G-21ST) as per ASTM-E384. The bond strength of coating was measured with the pull-off test method according to ASTM C-633-2013 standard at Metallizing Equipment Co. Pvt. Ltd., Jodhpur. The test consists of coating one face of a substrate fixture, bonding this coating to the face of a loading fixture, and subjecting this assembly of coating and fixtures to a tensile load normal to the plane of the coating. The commercially available epoxy resin adhesive provided by Metallizing Equipment Co. Pvt. Ltd., Jodhpur, was used for bonding the coated faces of the fixture, which has a nominal strength of about 70 MPa. For each coating, three test pieces were used and the average value was used as an indicator of the bond strength.

Accelerated Hot Corrosion Tests

All the specimens were wheel-polished before being subjected to accelerated hot corrosion runs. A coating of Na_2SO_4–60%V_2O_5 was applied on the preheated (250 °C) coated as well as bare specimens with a camel hairbrush with uniform thickness in the order of 3–5 mg/cm^2. Then the accelerated high-temperature oxidation studies were carried out under cyclic conditions for 50 cycles. Every cycle consisted of 60 min of heating at 900 °C in a silicon carbide tube furnace followed by 20 min of cooling in air at room temperature. Every specimen was positioned in an alumina boat separately and then inserted in the furnace. The cyclic study simulates the actual industrial environment where breakdown and shutdown occur frequently and provides the most brutal conditions for testing the materials. As per the literature available, the study of 50 cycles is well thought-out to be sufficient for attaining the steady-state oxidation for the material [20–23]. The studies were performed for the bare as well as coated specimens for the purpose of comparison. The weight change measurements were taken at the ending of each cycle with the help of Electronic Balance Model 06120 (Contech) with a sensitivity of 1 mg. The spalled scale was also included at the time of measuring weight change in order to determine the total rate of corrosion. Weight change data were analyzed to approximate the kinetics of corrosion. After the exposure, the corroded samples

were subjected to the XRD and FE-SEM/EDAX analyses for the surface as well as the cross-sectional analysis as per the procedure mentioned in Sect. 2.2.

Results

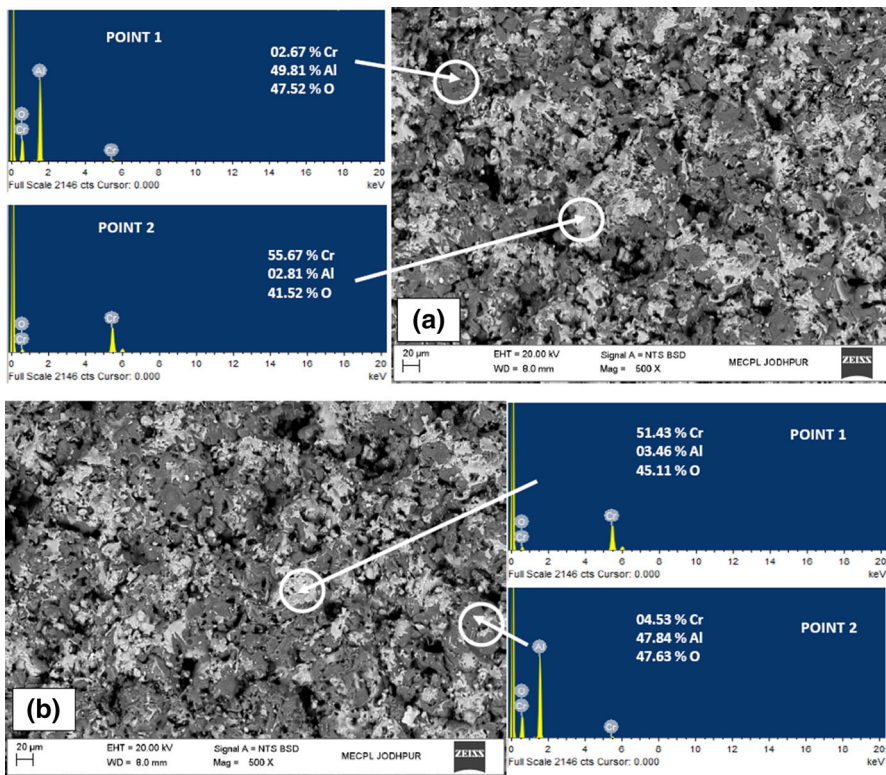### XRD Analysis of the As-Sprayed Coatings

The XRD diffractograms of the D-gun-sprayed Cr_2O_3–50% Al_2O_3 coating in as-sprayed conditions on ASTM-SA213-T-22 boiler steel and Fe-based superalloys Superfer 800H are depicted in Fig. 2 on reduced scale. The analysis indicates Cr_2O_3 and Al_2O_3 as the principal phases for the Cr_2O_3–50% Al_2O_3 coatings on both T-22 boiler steel and SF 800H.
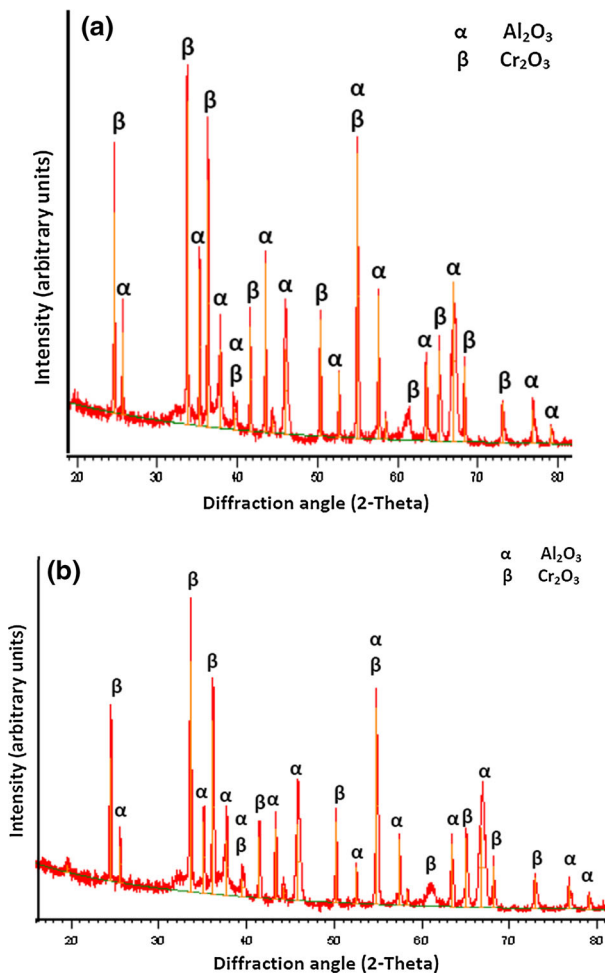
Fig. 2 X-ray diffraction pattern of D-gun-sprayed Cr_2O_3–50% Al_2O_3 coating on **a** ASTM-SA213-T-22 boiler steel, **b** Superfer 800H superalloy

SEM/EDAX Analysis of the As-Sprayed Coatings

The SEM micrographs along with EDS spectrum revealing the morphology of the surface in case of as-sprayed Cr_2O_3–50% Al_2O_3 coating on ASTM-SA213-T-22 boiler steel and Superfer 800H superalloy showing elemental composition (%) at selected points are shown in Fig. 3. The interlocked particles can be seen in the microstructure where most of the sprayed particles show flattened appearance due to the deformation during the coating process. The deformed shapes of particles are due to impact at higher velocities of particles during the D-gun spray process. The microscopic features indicate that the coatings in general are homogeneous and massive, free from cracks for both of the substrates (Fig. 3a, b). The EDAX analysis shows the domination of Cr and O in the light gray region (Point 2 in Fig. 3a and Point 1 in 3b) with small traces of Al, whereas the EDAX analysis of the dark gray region (Point 1 in Fig. 3a and Point 2 in 3b) of the coating reveals the domination of O and Al with small traces of Cr. This composition is almost approaching the composition of the sprayed powder.

Fig. 3 Surface scale morphology and EDAX analysis showing elemental composition (wt%) at selected points of D-gun-sprayed Cr_2O_3–50% Al_2O_3 coating on **a** ASTM-SA213-T-22 boiler steel, **b** Superfer 800H superalloy

Cross-Sectional Analysis of the As-Sprayed Coatings

The cross-sectional SEM image and X-ray mapping of the as-sprayed Cr_2O_3–50% Al_2O_3 coating on ASTM-SA213-T-22 boiler steel is shown in Fig. 4a. The bond coat and top coat of the coating have a dense appearance. In the vicinity of the coating/substrate interface, some superficial pores in the microstructure are present which are mostly concentrated. The X-ray mapping indicates the presence of Al and Cr along with O in the top coat, whereas the presence of Ni and Cr is revealed in the bond coat and no diffusion of iron from the substrate has been observed. The cross-sectional SEM image of the as-sprayed Cr_2O_3–50% Al_2O_3 coating on Superfer 800H superalloy is shown in Fig. 4b. The microstructure in general is similar to the microstructure in case of the T-22 substrate. The only difference that can be noted is that the interface seems to have lesser concentration of superficial pores in its surrounding area. The blending of the coating with the substrate seems excellent. The X-ray mapping is also similar to that for the T-22 substrate with the presence of Al, Cr and O in the top coat, whereas the presence of Ni and Cr is discovered in the bond coat with no diffusion of Fe from the substrate.

Coating Thickness for the Coatings

Average thickness of the coatings was measured from the cross-sectional SEM micrographs reported in Fig. 4. The average thickness measured for the Cr_2O_3–50% Al_2O_3 coating on ASTM-SA213-T-22 boiler steel was 588 µm (bond coat average thickness 256 µm and top coat average thickness 332 µm). In the case of the Cr_2O_3–50% Al_2O_3 coating on Superfer 800H, the coating thickness was observed as 500 µm (bond coat average thickness 204 µm and top coat average thickness 296 µm).

### Microhardness and Bond Strength of the As-Sprayed Coatings

The microhardness values of the Cr_2O_3–50% Al_2O_3 coating on ASTM-SA213-T-22 boiler steel and Superfer 800H superalloy are shown in Fig. 5, which depict the microhardness profiles all along the cross section of the coatings as a function of distance from the interface of coating and substrate. In case of Cr_2O_3–50% Al_2O_3-coated T-22 boiler steel, the microhardness values lies in the range of 702–881 Hv, with an average value of 776 Hv for the coating, whereas the substrate alloy has an average microhardness of the order 244 Hv. The microhardness value of Cr_2O_3–50% Al_2O_3 coating on Superfer 800H varies from 710 to 889 Hv with an average value of 783 Hv for the coating and 312 Hv for the substrate. The bond coat, i.e., Ni–20Cr, for both substrates has an average microhardness value of 191 Hv. The bond strength of the Cr_2O_3–50% Al_2O_3 coatings was measured on three specimens as per ASTM standard C633-2013 (as explained in Sect. 2.2). The coatings failed at the substrate–coating interface while remaining attached to the adhesive. Average bond strength of 48 MPa was observed.
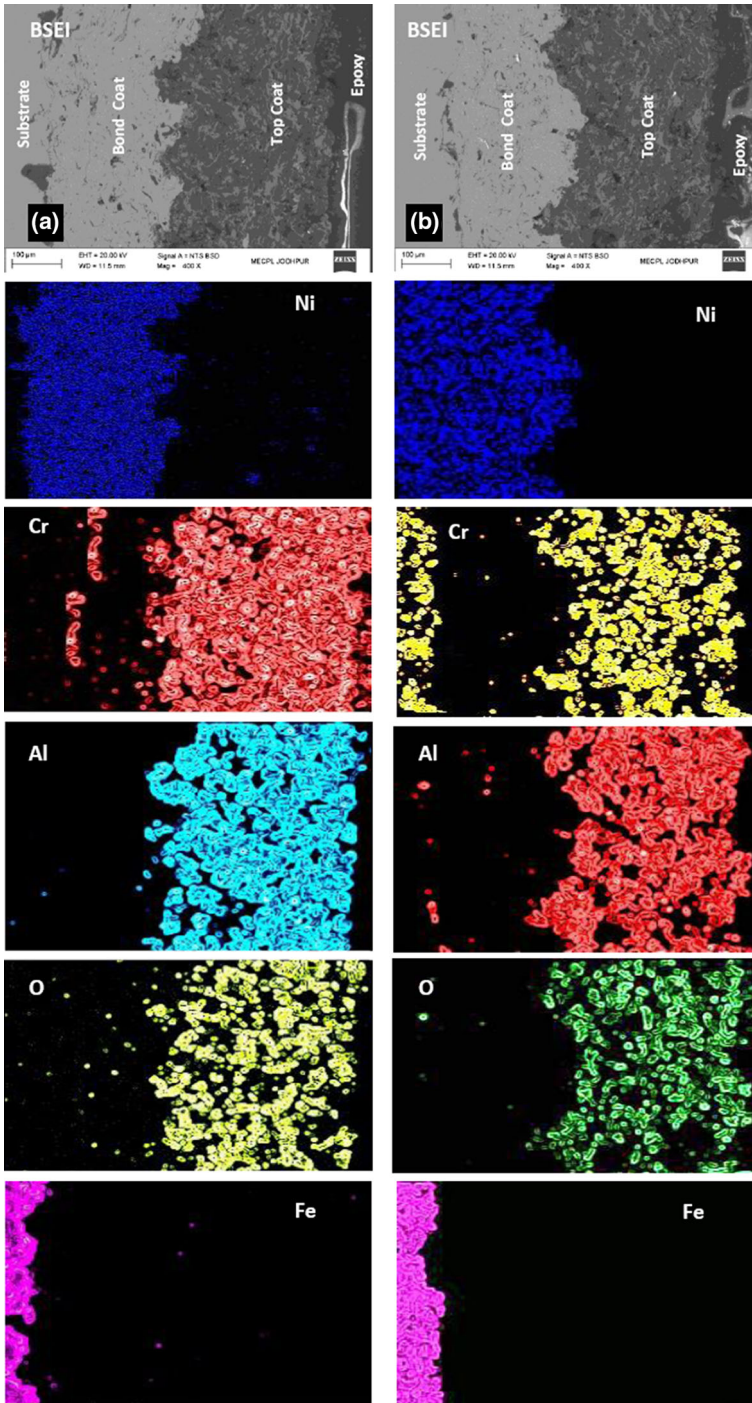
◀ **Fig. 4** SEM micrograph and X-ray mapping along the cross section of the D-gun-sprayed Cr_2O_3–50% Al_2O_3 coating on **a** ASTM-SA213-T-22 boiler steel, **b** Superfer 800H superalloy

Visual Examination of the Samples Subjected to Accelerated Hot Corrosion in Molten Salt

Macrographs of the bare and coated samples subjected to hot corrosion in Na_2SO_4–60% V_2O_5 molten salt environment at 900 °C for 50 cycles are represented in Fig. 6. In case of the bare T-22 boiler steel, a gray-colored flimsy scale appeared right from the first cycle. This bare steel has shown spalling of scale just after the fifth cycle, which was persistent till the end of 50th cycle. At the end of the study, asymmetrical and brittle scale was observed with yawning cracks with gray-colored surface appearance (Fig. 6a). Similarly, for the bare Superfer 800H superalloy a dark gray-colored scale appeared on the surface right from the second cycle, which turned to blackish green-colored surface along with a small light gray spot at the end of 50th cycle (Fig. 6b). The scale was seen intact with the substrate in general. In case of the Cr_2O_3–50% Al_2O_3-coated ASTM-SA213-T-22 boiler steel, the color of
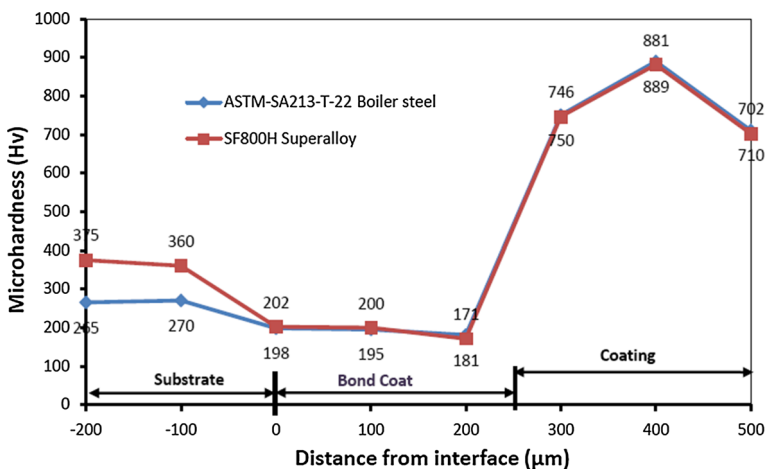
Fig. 5 Microhardness profile along the cross section of the D-gun-sprayed Cr_2O_3–50% Al_2O_3 coating on ASTM-SA213-T-22 boiler steel and Superfer 800H superalloy
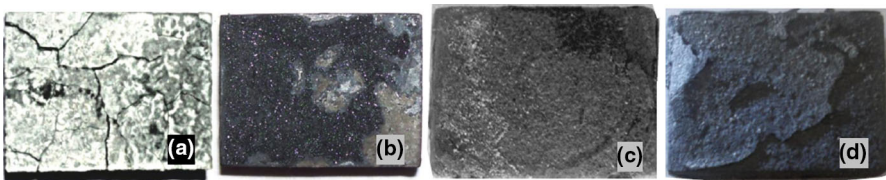
Fig. 6 Macrographs of the uncoated and coated samples subjected to hot corrosion in Na_2SO_4–60% V_2O_5 environment at 900 °C for 50 cycles: **a** uncoated T-22 steel; **b** uncoated Superfer 800H superalloy; **c** Cr_2O_3–50% Al_2O_3-coated ASTM-SA213-T-22 boiler steel; **d** Cr_2O_3–50% Al_2O_3-coated Superfer 800H superalloy

(a)

(b)

(c)
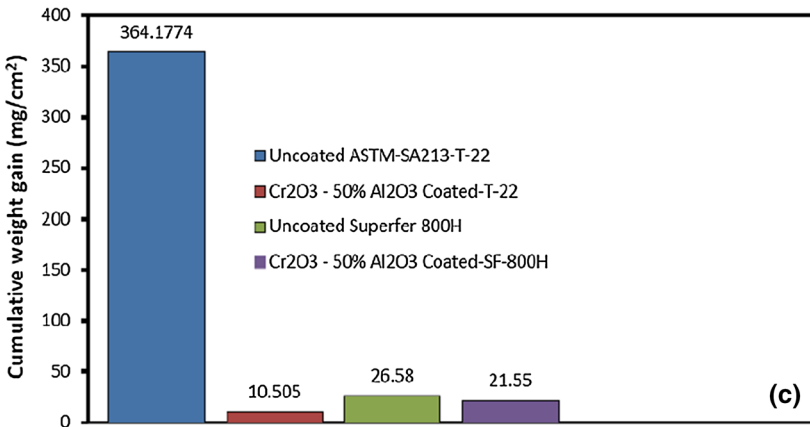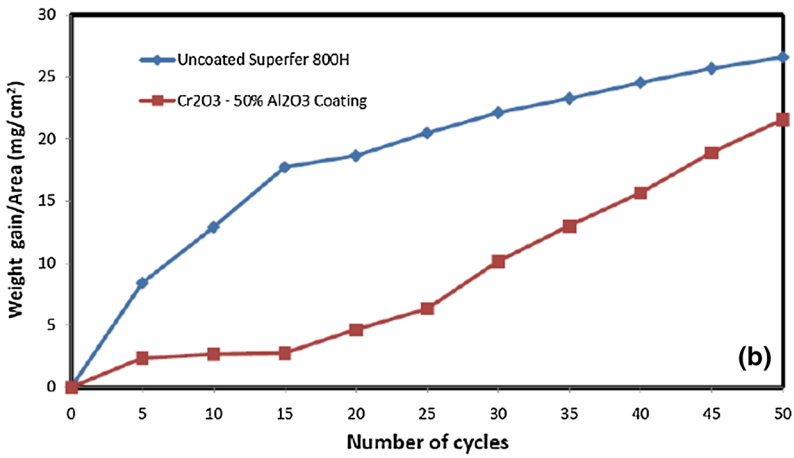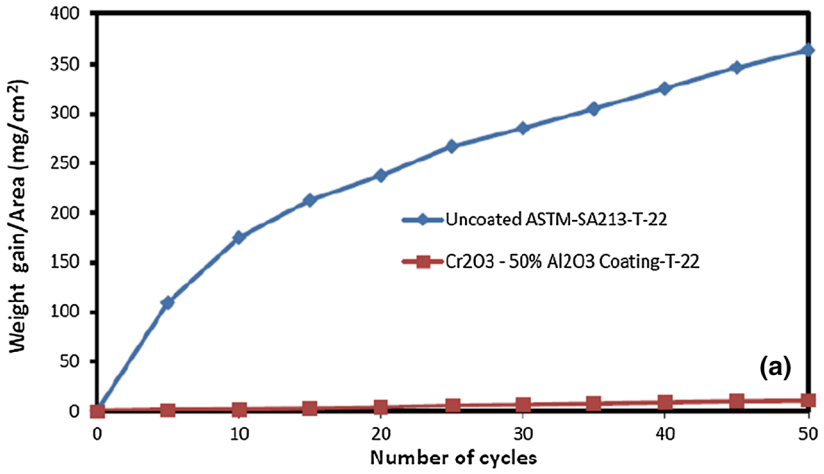
◄**Fig. 7** **a**, **b** Weight change/area versus number of cycles plot, **c** cumulative weight gain; for the uncoated and D-gun-sprayed Cr_2O_3–50% Al_2O_3 coating on ASTM-SA213-T-22 boiler steel and Superfer 800H superalloy subjected to hot corrosion in Na_2SO_4–60% V_2O_5 environment at 900 °C for 50 cycles

the specimen changed to gray after second cycle (Fig. 6c). The coating remained intact with the substrate in general. However, a minor spallation was seen at one edge of the specimen after 12th cycle and a small amount of powder was also found in the boat at the end of the 29th cycle. The surface of the specimen turned blackish gray at one edge (where marginal spallation was observed) along with light gray appearance of the remaining surface toward the end of the exposure. On the other hand, the color of the Cr_2O_3–50% Al_2O_3-coated Superfer 800H changed to dark gray after the very first cycle (Fig. 6d). The coating in general has shown the tendency of adherence with the substrate with no spallation tendency primarily up to 15th cycle. However, a shallow crack appeared on one edge of the specimen. The oxide scales were found to be smooth and intact with the substrate. After 20th cycle, there was engorgement at the edges of the specimen which subsequently led to the formation of some cracks on the edges as well as surface. The divergence between the coefficients of thermal expansion of the coating, oxide scales and the substrates may have caused the swelling and creation of cracks at the boundaries of the coated samples [20]. By the end of the 50th cycle, the specimen was blackish gray in color and appeared to be bloated with cracks all over. Loss of the material in the powder form was also observed by the end of the 38th cycle.

Weight Change Kinetics for the Accelerated Hot Corrosion Study

The data measured regarding change of weight during the accelerated hot corrosion investigation are shown in Fig. 7. Here, the weight change consists of a weight gain owning to the formation of the scales and a weight loss due to the spalling and dissolution of the scales and other corroded products. For comparison, hot corrosion of the uncoated alloys substrate was conducted in the same condition. Compared to the bare alloys, the weight gain of the coated specimens greatly decreased. The overall weight gain for bare T-22 steel (Fig. 7c) after 50 cycles of hot corrosion was found to be 364.17 mg/cm^2, and for bare Superfer 800H superalloy, it was 26.58 mg/cm^2. Therefore, as far as the weight gain is concerned, the corrosion resistance of Superfer 800H superalloy has been proved be to much more than T-22 boiler steel in the aggressive environment under study. In the case of the Cr_2O_3–50% Al_2O_3-coated alloys, it can be observed from the plots (Fig. 7a, b) that the essential protection against the high-temperature corrosion in hostile molten salt environment has been provided by the Cr_2O_3–50% Al_2O_3 coating as the weight gain values for the bare alloys are very much higher than those for their respective coated counterparts. The concluding weight gain for the Cr_2O_3–50% Al_2O_3-coated T-22 boiler steel is 10.50 mg/cm^2, and for the Superfer 800H superalloy substrate alloy, it is 21.55 mg/cm^2. Thus, it can be inferred from the weight change graphs that the weight gain in case of coated T-22 steel is much lesser than the bare T-22 steel and similar trend was observed in case of bare and coated superalloy. The plots for the bare samples have shown higher weight gain during initial cycles which was

followed by gradual gain in weight. In case of Cr_2O_3–50% Al_2O_3-coated T-22 steel, the weight change is almost negligible throughout the study, whereas in case of Cr_2O_3–50% Al_2O_3-coated Superfer 800H superalloy, the weight gain abruptly increased after 25th cycle.

The (weight gain/area)^2 versus number of cycles plot (Fig. 8) is shown for all the samples to establish conformance with the parabolic rate law. Table 3 shows the value of the parabolic rate constant, i.e., K_p, which was obtained from the slope of the linear regression fitted line (cumulative weight gain per unit area)^2 versus number of cycles (Fig. 8). It is clear from the graph that in spite of some
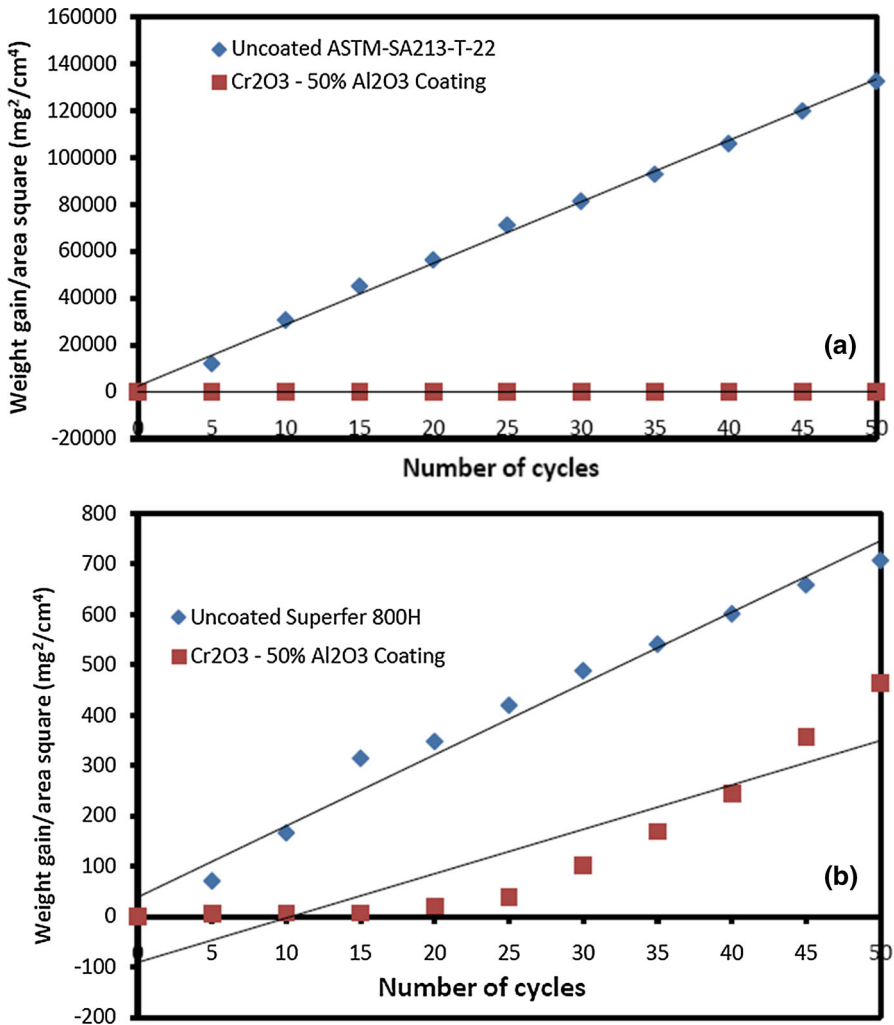
Fig. 8 (Weight change/area)^2 versus number of cycles plot for the uncoated and D-gun-sprayed Cr_2O_3–50% Al_2O_3 coating on **a** ASTM-SA213-T-22 boiler steel and **b** Superfer 800H superalloy, subjected to hot corrosion in Na_2SO_4–60% V_2O_5 environment at 900 °C for 50 cycles
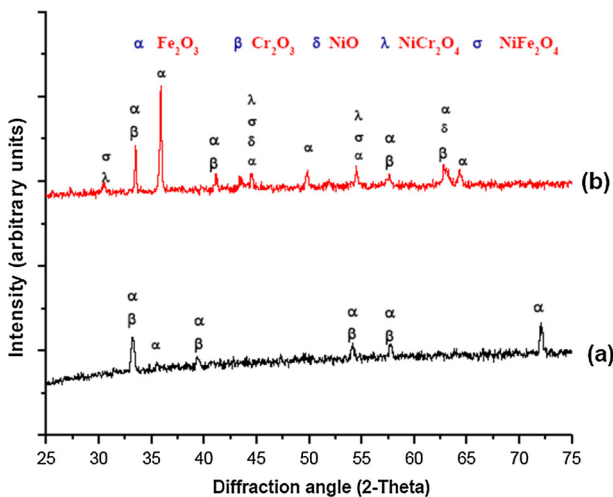
Table 3 Parabolic rate constant "K_p" values of the uncoated and coated samples subjected to hot corrosion in Na_2SO_4–60% V_2O_5 environment at 900 °C for 50 cycles

Uncoated and coated alloy	$K_p \times 10^{-08}$ g^2 cm^{-4} s^{-1}
Uncoated T-22 boiler steel	72.77
Uncoated SF 800H superalloy	00.39
Cr_2O_3–50% Al_2O_3-coated T-22 boiler steel	00.06
Cr_2O_3–50% Al_2O_3-coated SF 800H superalloy	00.24

fluctuations, the data conform to the parabolic rate law to tolerable limit for both the bare alloys. Further, both the coated specimens have also followed the parabolic rate law for the entire 50 cycles of study, which can be inferred from the plots (Fig. 8). However, a deviation was observed after 15th cycle in the case of the Cr_2O_3–50% Al_2O_3-coated Superfer 800H superalloy. The parabolic rate constant (K_p) value for both the coated substrate is lesser then their uncoated counterpart. The minimum value of parabolic rate constant (K_p) was observed in case of Cr_2O_3–50% Al_2O_3-coated T-22 boiler steel, i.e., 0.066×10^{-08} g^2 cm^{-4} s^{-1}, and maximum for uncoated T-22 boiler steel, i.e., 72.77×10^{-08} g^2 cm^{-4} s^{-1}.

XRD Examination of the Scale

The XRD diffractograms (on reduced scale) of the oxide scale for the bare alloy samples exposed to the hot corrosion at 900 °C for 50 cycles are depicted in Fig. 9. The scale of uncoated T-22 steel indicated mainly the presence of Fe_2O_{-3} and Cr_2O_3 phases (Fig. 9a), whereas in case of uncoated Superfer 800H superalloy, the main oxide phases identified are Fe_2O_3, Cr_2O_3, NiO, $NiCr_2O_4$ and $NiFe_2O_4$ (Fig. 9b).
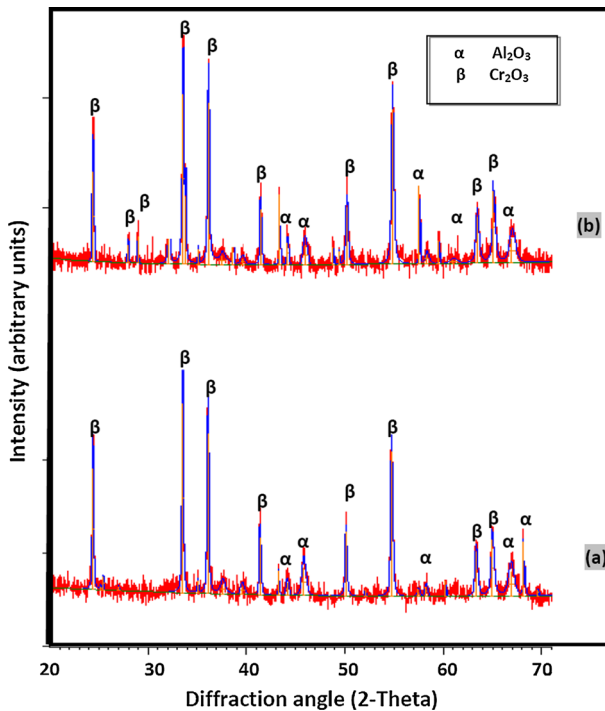

Fig. 9 X-ray diffraction pattern for the uncoated samples subjected to hot corrosion in Na_2SO_4–60% V_2O_5 environment at 900 °C for 50 cycles: *a* uncoated T-22 steel; *b* uncoated Superfer 800H superalloy

XRD diffractograms (on reduced scale) for the Cr_2O_3–50% Al_2O_3-coated alloys subjected to high-temperature oxidation in Na_2SO_4–60%V_2O_5 molten salt at 900 °C for 50 cycles are depicted in Fig. 10. The top scale indicated mainly the presence of Al_2O_{-3} and Cr_2O_3 phases.

Investigation of the Scale with SEM/EDAX

Scale's Surface Morphology

Figure 11 shows the SEM micrographs indicating morphology of the bare alloys after being subjected to the hot corrosion testing in molten salt environment. In the case of bare T-22 boiler steel (Fig. 11a), the surface micrograph shows noteworthy spalling of its top layer and the oxide scale is badly damaged. The surface scale shows twisted, out-of-shape and spalled grains-like microstructure. The exposed portion of the scale gives the impression to be impenetrable and adherent. The scale has an amorphous appearance at some other locations. The EDAX scrutiny reveals that the scale is rich in Fe and O, in general, which suggests the likelihood of formation of iron oxide, i.e., Fe_2O_3. Point 1 indicates the presence of Cr, which also predicts the possibility of formation of chromium oxide, i.e., Cr_2O_3. The grains are

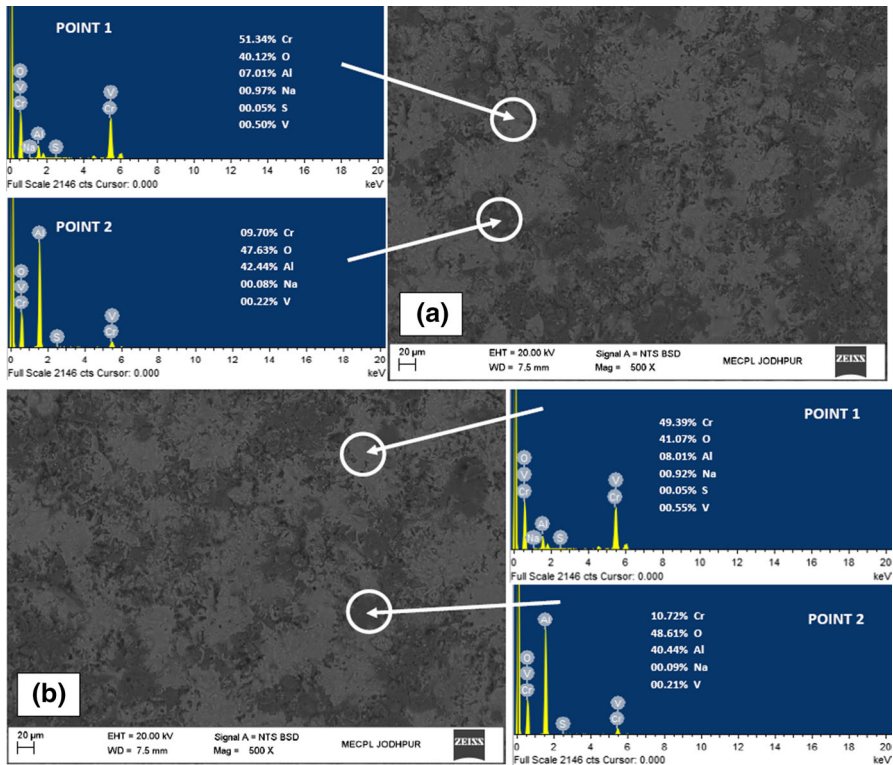**Fig. 10** X-ray diffraction pattern for the D-gun-sprayed Cr_2O_3–50% Al_2O_3-coated samples subjected to hot corrosion in Na_2SO_4–60% V_2O_5 environment at 900 °C for 50 cycles for substrate: *a* T-22 steel; *b* Superfer 800H superalloy
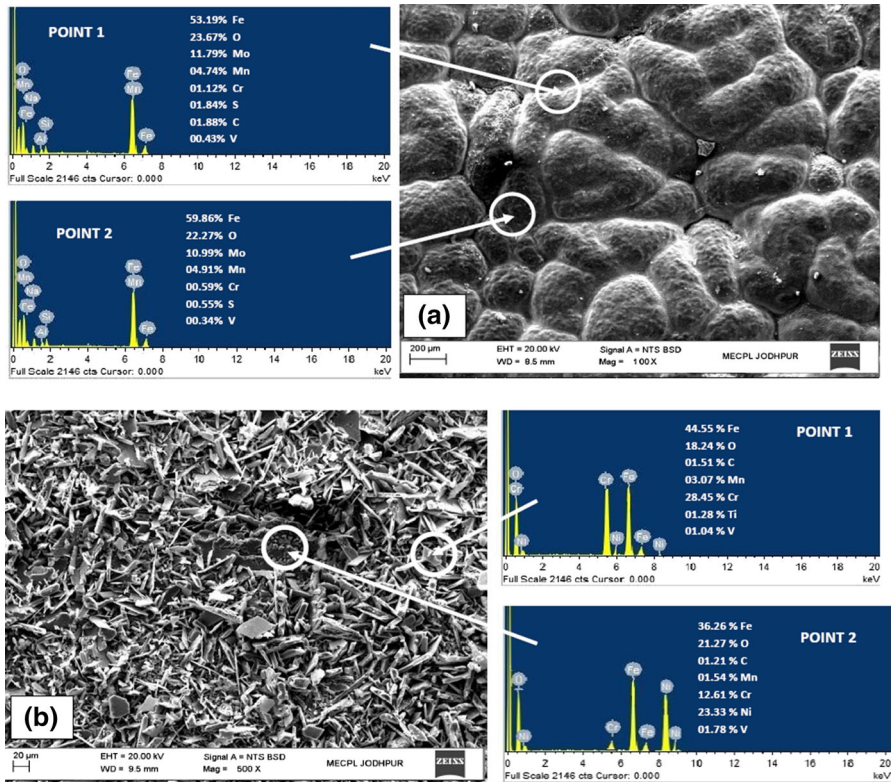
Fig. 11 Surface scale morphology and EDAX analysis showing elemental composition (wt%) at selected points for the uncoated samples subjected to hot corrosion in Na_2SO_4–60% V_2O_5 environment at 900 °C for 50 cycles: **a** uncoated T-22 steel; **b** uncoated Superfer 800H superalloy

of dark gray color (Point 1), and boundaries are whitish in appearance (Point 2). On the other hand, in the case of the uncoated Superfer 800H superalloy (Fig. 11b), the micrograph shows small needles dispersed in matrix-like structures. The top scale is rich in Fe, Ni, Cr and O. Small amounts of Al, Mn, Ti and C are also present. The EDAX point analysis shows that the concentration of Fe, O and Cr is more in needles, whereas the concentration of Fe, O and Ni is more in base matrix along with Cr. Small amounts of Mn, C and Ti as indicated by Points 1 and 2 have also been observed. The micrograph for the Cr_2O_3–50% Al_2O_3-coated alloys after being subjected to the hot corrosion tests reveals the formation of a homogeneous, massive and free from cracks structure as depicted in Fig. 12. The surface appearance at microscopic level is almost identical. The EDAX analysis shows the domination of Cr and O in the light gray region (Point 1 in Fig. 12a and Point 1 in 12b) with small traces of Al, whereas the EDAX analysis of the dark gray region (Point 2 in Fig. 12a and Point 2 in 12b) of the coating reveals the domination of O and Al with small traces of Cr.

Fig. 12 Surface scale morphology and EDAX analysis showing elemental composition (wt%) at selected points for the D-gun-sprayed Cr_2O_3–50% Al_2O_3-coated samples subjected to hot corrosion in Na_2SO_4–60% V_2O_5 environment at 900 °C for 50 cycles: **a** T-22 steel substrate; **b** Superfer 800H superalloy substrate

Analysis of the Oxide Scale Along the Cross Section of the Sample

Figure 13a shows the SEM micrograph of the cross section of the corroded bare T-22 boiler steel alloy. A chunky oxide scale is discovered which is supposed to have developed in the form of laminar layers. There is a considerable existence of cracks, some of which are perpendicular to the surface of the steel, while some are parallel. In the vicinity of the oxide–matrix interface, significant corrosion damage has been observed. A dense scale containing mainly iron and oxygen with some amount of chromium is being indicated by the X-ray mapping analysis. Chromium is present in the oxide scale in the form of some parallel thin bands along with oxygen. The SEM micrograph of oxide scale for the corroded uncoated Superfer 800H superalloy is depicted in Fig. 13b. The X-ray mapping analysis for a fraction of oxide scale shows nickel-dominating continuous scale, which contain substantial amounts of iron and oxygen. Chromium and oxygen have shown their co-presence in the form of some pockets in the scale and at the scale/substrate interface, where iron and nickel are completely missing. On the other hand, the oxide scales for the
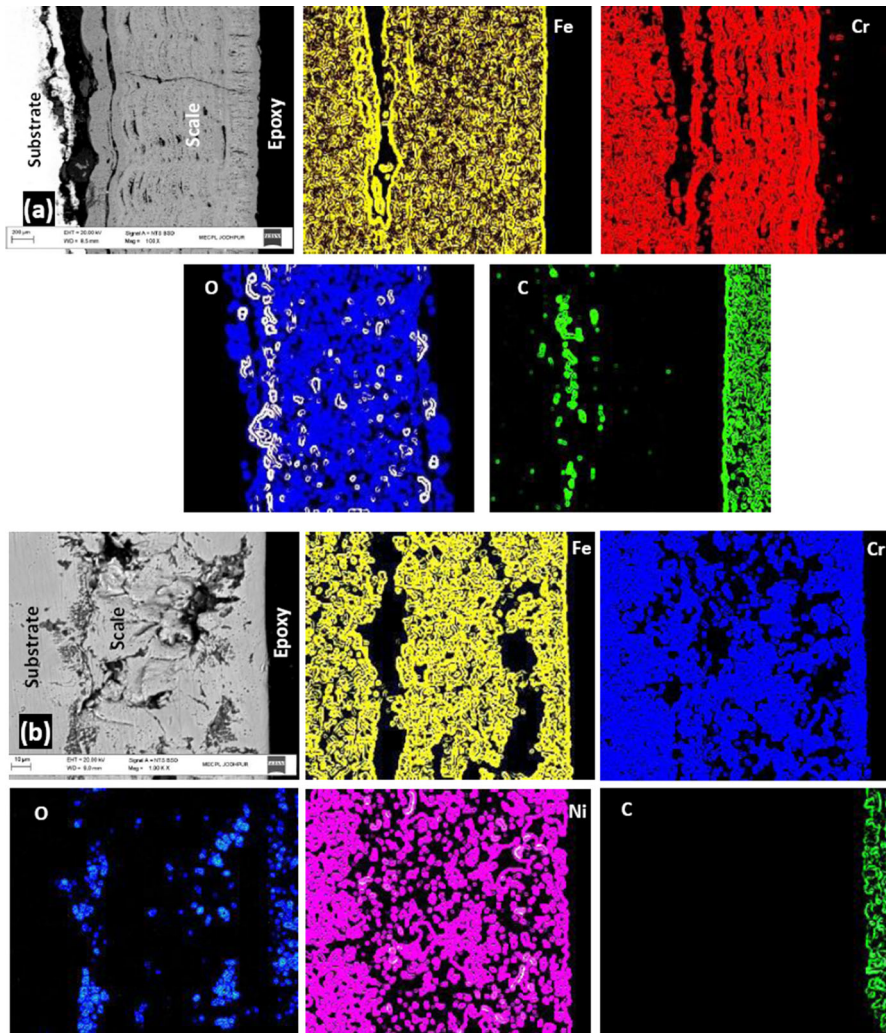
Fig. 13 SEM micrograph and X-ray mapping along the cross section for the uncoated samples subjected to hot corrosion in Na_2SO_4–60% V_2O_5 environment at 900 °C for 50 cycles: **a** uncoated T-22 steel; **b** uncoated Superfer 800H superalloy

Cr_2O_3–50% Al_2O_3-coated alloys after being subjected to the hot corrosion tests are found to be adherent with no damage for the interface of substrate and scale, as shown in Fig. 14. The scale seems to be dense in manifestation having laminar morphology. No cracks have been observed along/perpendicular to the thickness of the scales. The absence of corrosive species at the point of coating/substrate interface indicates that during the hot corrosion runs, the substrate alloys remained unaltered. The top coat is mainly rich in Cr and Al along with O, whereas the bond coat indicates the rich presence of Cr and Ni with no substrate species, i.e., Fe for
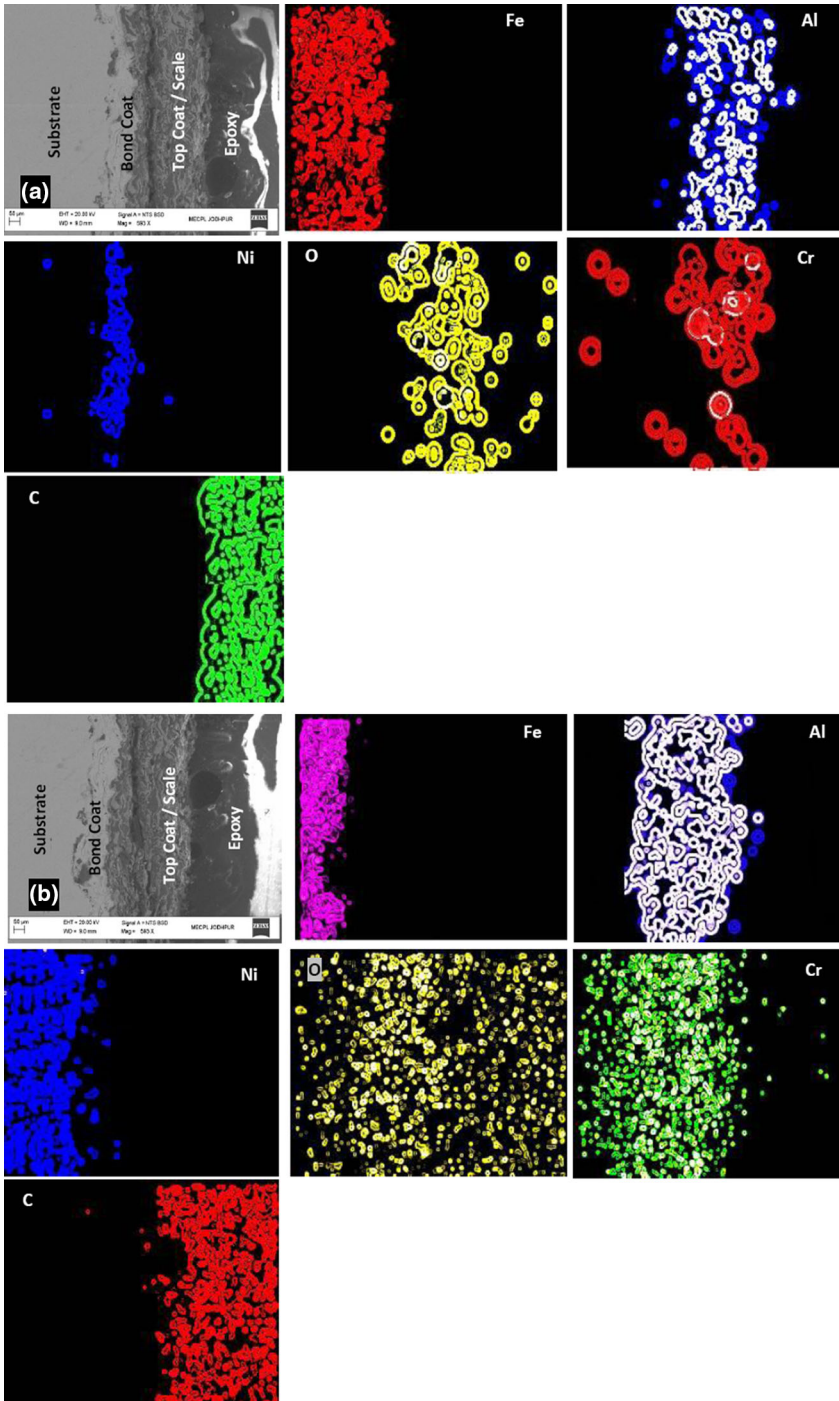
both substrates (Fig. 14a, b). This means no diffusion of the substrate elements has taken place in the coated samples after hot corrosion run. It is fascinating to note that the diffusion of O is not very noteworthy along the coating thickness in both the coated samples under study. Thus, we can say that the coatings are very much effective to resist the penetration of the oxidizing species toward the base steels.

Discussion

The D-gun spray process provides the opportunity of deposition of Cr_2O_3–50% Al_2O_3 coating on the T-22 and Superfer 800H iron-based alloys; the coating has virtually adherent, homogeneous and dense microstructure. The microscopic features indicate that the coatings are homogeneous, massive and free from cracks for both the substrates (Fig. 3a, b). The microhardness values for both the coatings have been found to be very high as compared to the substrates (Fig. 5). The microhardness values for the Cr_2O_3–50% Al_2O_3-coated T-22 boiler steel lie in the range of 702–881 Hv, while for Cr_2O_3–50% Al_2O_3 coating on Superfer 800H alloy, the hardness value varies from 710 to 889 Hv. The bond coat, i.e., Ni–20Cr, for both substrates has average microhardness value of 191 Hv. Some variations observed in hardness values of the coating may be caused by the presence of porosity, un-melted and incompletely melted particles. Further, a slightly higher hardness value has been observed as compared to the bare substrates, near the coating–substrate interface. This might be due to the sandblasting of the substrates prior to the coating process which causes work hardening effect [24–28]. Also the minor diffusion of elements from the substrate to coating may have created difference in the microhardness values of the coating on different substrate.

Cr_2O_3 and Al_2O_3 have been identified as the prominent phases by the XRD analysis (Fig. 3) for as-sprayed Cr_2O_3–50% Al_2O_3 coating on the T-22 and Superfer 800H Fe-based alloys by D-gun process. This is further certified by the EDAX analysis which shows the dominance of Al, Cr and O in the coating (Fig. 3). The SEM/EDAX examination of the cross section (Fig. 4) for both the coatings shows that the interface between the coating and the substrate is reasonably flawless with minor pores and voids. The bond coat and top coat of the coating on the whole have a thick appearance. The presence of some shallow pores in the microstructure has been observed, which are mostly concentrated in the vicinities of the interface of coating and substrate. The X-ray mapping indicates the presence of Al and Cr along with O in the top coat, whereas the presence of Ni and Cr is revealed in the bond coat and no diffusion of iron from the substrate has been observed.

Both the bare alloys have shown rapid weight gain (Fig. 7) after exposure to the selected molten salt environment for 50 cycles at 900 °C, whereas the Cr_2O_3–50% Al_2O_3-coated T-22 and Superfer 800H Fe-based alloys showed resistance to weight gain. The weight change graph (Fig. 7) shows that the weight increases incessantly,

although the pace of increase is high throughout the initial period of exposure. The rapid increase in the weight gain during the initial period of exposure to Na_2SO_4–60%V_2O_5 molten salt environment at 900 °C can be attributed to the possible formation of $NaVO_3$. Kolta et al. [29] proposed that in the temperature range of 900 °C, the Na_2SO_4 and V_2O_5 will combine to form $NaVO_3$, as represented by Eq. (1) having a melting point of 610 °C.

$$Na_2SO_4 + V_2O_5 = 2NaVO_3(l) + SO_2 + 1/2O_2 \qquad (1)$$
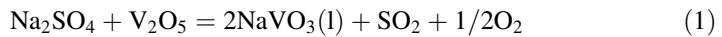
This $NaVO_3$ acts as a catalyst and also serves as an oxygen carrier to the base alloy through the open pores present on the surface, which will lead to the rapid oxidation of the base elements of the substrate to form a protective oxide scale. There may be simultaneous dissolution of protective oxide Cr_2O_3 in the molten salt due to the reaction [30–34]:

$$Cr_2O_3 + 4NaVO_3 + 3/2O_2 = 2Na_2CrO_4 + 2V_2O_5 \qquad (2)$$
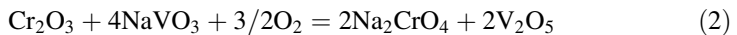
The Na_2CrO_4 gets evaporated as a gas. The rapid increase in the weight gain during the initial period was also reported by Sidhu et al. [35–37], Singh et al. [1, 38], Tiwari and Prakash [39–41], Chawla et al. [42–45] and Ul-amid [21] during their studies on the hot corrosion of alloys. Also, the higher weight gain during the first few cycles can be attributed to the rapid formation of oxides at the splat boundaries (in case of coatings) and within the open pores due to the penetration of the oxidizing species. Once the oxides are formed at places of porosity and splat boundaries, the coating becomes dense and the diffusion of oxidizing species to the internal portions of the coatings gets slowed down and the growth of the oxides becomes limited mainly to the surface of the specimens. This, in turn, will make the weight gain and hence the oxidation rate steady with the further progress of exposure time [35, 46]. Intense spalling, high corrosion rate, irregular and fragile scale with deep cracks and gray color surface appearance were observed for bare T-22 alloy (Fig. 6a). The corrosion rate was higher in the case of T-22 alloy. The severe spalling of the scale for similar type of steel, i.e., T-22 steel, was also observed by Singh [47], Bala et al. [48] and Chawla et al. [42] during hot corrosion study in Na_2SO_4–60%V_2O_5 environment at 900 °C. The surface XRD analysis (Fig. 9a) indicated the formation of Fe_2O_3 as the main constituent of the top scale in bare T-22 alloy after the hot corrosion in Na_2SO_4–60%V_2O_5 environment at 900 °C. The formation of Fe_2O_3 has also been reported by Shi [49] during the oxidation of iron by Na_2SO_4 at 750 °C. Similar results were reported by Tiwari and Prakash [39] and Singh et al. [23] during hot corrosion of iron-based superalloy in Na_2SO_4–60%V_2O_5 environment at 900 °C. The weak peaks of Cr_2O_3 along with major peaks of Fe_2O_3 in the case of bare T-22 alloy may be due to the presence of Cr in the alloy steel. Similar results have been reported by Chawla et al. [42, 43] and Singh [47]. The XRD results are further supported by the surface EDAX analysis (Fig. 11a). The X-ray mapping analysis (Fig. 13a) of the cross section also shows the presence of Fe along with oxygen in the outer scale in the case of the corroded T-22 boiler steel. Small amounts of Cr have also been noticed in the subscale. The presence of Cr might have led to control the oxidation rate in the case of T-22 alloy

as chromium is present in the oxide scale in the form of some parallel thin bands along with oxygen (Fig. 13a). Similar results were reported by Sididue et al. [50]. The authors have reported that Fe–Cr alloys in oxygen at higher temperature (950–1050 °C) form spinel ($FeCr_2O_4$ and Cr_2O_3) on the inner side and Fe_2O_3 on the outer side of the scale, whereas for the bare Superfer 800H superalloy, a dark gray-colored scale appeared on the surface right from the second cycle, which turned to blackish green-colored surface along with a small light gray spot at the end of 50th cycle (Fig. 6b). The scale was found to be intact with the substrate in general. Similar type of behavior has also been reported by Chawla et al. [44], Kamal et al. [8], Sachs [51] and Singh et al. [23]. The authors have explained that intensive spalling of the scale as observed in case of Superfer 800H can be attributed to severe strain developed because of Fe_2O_3 precipitation from the liquid phase and inter diffusion of intermediate layers of iron oxide. Further, the presence of three different phases in a thin layer would impose severe strain on the film, which may result in cracking and exfoliation of the scale. The cracks may have allowed the aggressive liquid phase to reach the metal substrate [51]. The surface XRD analysis (Fig. 9b) revealed the main oxide phases as Fe_2O_3, Cr_2O_3, NiO, $NiCr_2O_4$ and $NiFe_2O_4$ (Fig. 9b). Similar results have been reported by Kamal et al. [8] and Singh et al. [23]. The XRD results are further supported by the surface EDAX analysis (Fig. 11b). The X-ray mapping analysis of the cross section of the corroded Superfer 800H alloy also shows Fe and O elements in its oxide scale along with Ni and Cr, which predicts the formation of Fe_2O_3. The formation of Fe_2O_3 in the scale has been reported to be non-protective by Das et al. [52] during their hot corrosion study on Fe_3Al-based iron aluminized in Na_2SO_4 atmosphere. That is perhaps why both the uncoated alloys suffered accelerated hot corrosion. Both the uncoated alloys showed near-parabolic behavior with a transition in their K_p values (Table 3). The parabolic rate constant K_p was obtained from the slope of the linear regression fitted line (cumulative weight gain/area)^2 versus number of cycles. It is clear that in spite of some fluctuations in the data for the uncoated alloys, the data conform to the parabolic rate law to an acceptable limit for both the alloys. The maximum value of parabolic rate constant (K_p) was observed in case of uncoated T-22 boiler steel, i.e., 72.77×10^{-08} g^2 cm^{-4} s^{-1}. In terms of overall weight gain, Superfer 800H superalloy has been proved be to much more corrosion resistant in the aggressive environment under study than T-22 boiler steel.

The Cr_2O_3–50% Al_2O_3 D-gun spray-coated alloys have shown better corrosion resistance than their uncoated counterparts. The Cr_2O_3–50% Al_2O_3 coating was successful to reduce the corrosion rate of the T-22 steel by 97%, in terms of overall weight gains, whereas the reduction was 19% for the Superfer 800H alloy (Fig. 7c). In case of Cr_2O_3–50% Al_2O_3-coated T-22 alloy, the weight change was almost negligible throughout the study, whereas in case of Cr_2O_3–50% Al_2O_3-coated Superfer 800H superalloy, the weight gain abruptly increased after 25th cycle but remained lesser than the bare counterpart. The oxides formed on iron-, nickel- and cobalt-based alloys are not sufficiently protective above 500 °C and are alloyed with chromium, aluminum or silicon to form more protective oxides (scales), i.e., chromia, alumina or silica, respectively. But, in case of high-alloy materials which could be capable of forming more protective oxide layer when exposed to high-

temperature oxidizing environment, the component size and complexity as well as the rather limited ratio of improved corrosion resistance versus increased costs in most cases exclude solutions based on bulk materials [53]. The Cr_2O_3 and Al_2O_3 are generally regarded as the best protective oxides, with relatively slow diffusion compared to other oxides [54]. As reported by Schutze et al. [53], a common feature of Al-based coatings is that they act as a reservoir phase for the formation of protective and slow-growing Al-based oxide scales by reaction with the operation environment, thus providing an environment barrier against the ingress of more aggressive species down to the metal to be protected and slowing down metal consumption rates by the oxidation process itself.

In hot corrosion process, when Na_2SO_4 is present, the following reaction usually also takes place [55, 56]:

$$Na_2SO_4 = Na_2O + SO_3 = Na_2O + SO_2 + 1/2O_2 \qquad (3)$$
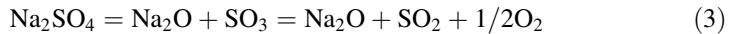
Since Al_2O_3 is stable in Na_2SO_4 and fluxing of Al_2O_3 scale by a molten salt is strongly dependent on oxygen ion activity of the molten salt [57]. With the increase of Na_2O, an oxide ion activity can be reached at which the reaction: $Al_2O_3 + O^{2-} = 2AlO_2^-$ occurs. The basic fluxing of the Al_2O_3 scale caused the accelerated oxidation, so the mass gain increases linearly after 25th cycle in case of Cr_2O_3–50% Al_2O_3-coated Superfer 800H superalloy (Fig. 7b), but this was not observed in case of Cr_2O_3–50% Al_2O_3-coated T-22 alloy (Fig. 7a). Also due to presence of Na_2SO_4 at the initial stages, Cr_2O_3 is not stable on the alloy surface because the oxide ion concentration of Na_2SO_4 is sufficient for the formation of chromate ions:

$$Cr_2O_3 + 3Na_2O + 1/2O_2 = 2Na_2CrO_4 \qquad (4)$$

This causes the initial hot corrosion rate to be high. When the oxide ion activity of the sulfate is quickly reduced by reaction with Cr_2O_3 to values where Cr_2O_3 is stable on the alloy surface, the oxides of Cr and Al, i.e., Cr_2O_3 and Al_2O_3, become stable and oxidation takes place much the same as the absence of Na_2SO_4 [57].

Furthermore, both the coated steels followed the parabolic law, which indicates that the scales formed have shown the tendency to act as diffusion barrier to corrosive species. This shows the corrosion protective behavior of the Cr_2O_3–50% Al_2O_3 coating. The minimum value of parabolic rate constant (K_p) was observed in case of Cr_2O_3–50% Al_2O_3-coated T-22 boiler steel, i.e., 0.066×10^{-08} g^2 cm^{-4} s^{-1}, and maximum for uncoated T-22 boiler steel, i.e., 72.77×10^{-08} g^2 cm^{-4} s^{-1}. A deviation in the parabolic rate constant (K_p) value was observed at the end of the 15th cycle in the case of the Cr_2O_3–50% Al_2O_3-coated Superfer 800H superalloy. The Cr_2O_3–50% Al_2O_3-coated T-22 boiler steel has shown lower corrosion rate than the coated Superfer 800H alloy. It is well known that the performance of thermal sprayed coatings in high-temperature corrosive environment depends upon the several factors such as porosity, inclusions, oxides and size and shape of the splat microstructures as reported in the literature [55].

The top scale indicated mainly the presence of Al_2O_3 and Cr_2O_3 phases in the surface XRD analysis (Fig. 10) for the Cr_2O_3–50% Al_2O_3-coated alloys after hot corrosion studies. No sign of diffusion of the substrate elements has been identified

in the surface XRD analysis. The surface EDAX analysis (Fig. 12) also supports the XRD analysis results that Al, Cr and O have been identified as the main phases by the analysis. The same has been indicated by the X-ray mapping analysis (Fig. 14) for both of the coated specimens. No sign of diffusion has been identified in the cross-sectional analysis. The cross-sectional X-ray mapping analysis also reveals richness of Al, Cr and O in the outer scale of the coated alloys (Fig. 14) with clearly visible bond coat of Ni and Cr as inner layer on the substrate, which may explain somewhat higher corrosion resistance of the coated alloys when compared to their uncoated counterparts. The presence of Cr_2O_3 and Al_2O_3 phases in the oxide scales of the coated alloys provides shield to the base metal against any diffusion of oxidizing species. These oxide phases are thermodynamically stable [8] up to very high temperatures due to its high melting points, and it forms a dense, continuous and adherent layers that grow relatively slow [59]. The scale of this type forms a solid diffusion barrier that inhibits interaction of oxygen of underlying coating. Coatings are usually designed in such a way that on exposure to reactive environments, the selective oxidation of an element occurs to form a protective oxide scale such as Cr_2O_3, Al_2O_3 or SiO_2 [18]. The formation and growth of oxide scales are determined by an extensive range of parameters, including the alloy composition and the oxidizing environment. Therefore, it may be very difficult to establish a continuous, protective scale under some conditions [60]. These oxides are very protective as reported by Ul-Hamid [21] and Sundarajan et al. [61]. Moreover, as seen from the cross-sectional analysis of the coated steels, no O has penetrated in the substrate, which means the chances of the internal oxidation are meager. Therefore, based on the present investigation, it can be concluded that D-gun-sprayed Cr_2O_3–50% Al_2O_3 coating can provide a very good hot corrosion resistance to the T-22 boiler steel and Superfer 800H alloy at high temperatures.

Conclusions

- Cr_2O_3–50% Al_2O_3 ceramic powders were successfully sprayed on Fe-based alloys, namely T-22 boiler steel and Superfer 800H by the D-gun spray process, which resulted in a coating with nearly uniform, adherent and dense microstructure.
- Cr_2O_3–50% Al_2O_3 D-gun spray coatings were found to have significantly higher microhardness (in the range 702–889 Hv) in comparison with the selected base alloys.
- The bare T-22 boiler steel showed enormous weight gain, high corrosion rate, irregular and fragile scale with deep cracks, gray color surface appearance and substantial spallation of their oxide scales during hot corrosion studies in the aggressive environment of Na_2SO_4–60%V_2O_5 environment at 900 °C, whereas for the bare Superfer 800H superalloy, a dark gray-colored scale appeared on the surface right from the second cycle, which turned to blackish green-colored surface along with a small light gray spot at the end of 50th cycle. The scale was found to be intact with the substrate in general.

- The D-gun-sprayed Cr_2O_3–50% Al_2O_3 coating on two different substrates when subjected to hot corrosion in Na_2SO_4–60%V_2O_5 environment at 900 °C was found to be successful in maintaining its adherence with the substrate steels. The oxide scales were also found to be intact, and there was no indication of spalling in both the cases.

- The Cr_2O_3–50% Al_2O_3 coating was successful to reduce the corrosion rate of the T-22 steel by 97%, in terms of overall weight gains, whereas the reduction was 19% for the Superfer 800H alloy. In case of Cr_2O_3–50% Al_2O_3-coated T-22 alloy, the weight change is almost negligible throughout the study, whereas in case of Cr_2O_3–50% Al_2O_3-coated Superfer 800H superalloy, the weight gain abruptly increased after 25th cycle, but remained lesser than the bare counterpart.

- Both the coated steels after exposure to molten salt-induced cyclic oxidation have shown protection to the substrate due to the presence of alumina and chromia in their oxide scales, which are reported to be protective against hot corrosion. In case of Cr_2O_3–50% Al_2O_3-coated T-22 alloy, the weight change was almost negligible throughout the study.

- The D-gun spray-coated Cr_2O_3–50% Al_2O_3 coating was found to be very useful in developing hot corrosion resistance in T-22 and Superfer 800H alloys.

References

1. H. Singh, D. Puri, and S. Prakash, *Metallurgical and Materials Transactions A: Physical Metallurgy and Materials Science* **36**, 1007 (2005).
2. N. Eliaz, G. Shemesh, and R. M. Latenision, *Engineering Failure Analysis* **9**, 31 (2002).
3. A.S. Khanna, *High Temperature Oxidation-Basics in 'Introduction to High Temperature Oxidation and Corrosion'* (ASM International, USA, 2002)
4. J. B. Marriott, *Mater Design* **11**, 122 (1990).
5. S. Prakash, S. Singh, B.S. Sidhu, and A. Madeshia, Tube Failures in Coal Fired Boilers, in *Proceedings of the National Seminar on Advances in Material and Processing*, 9–10th November (IIT, Roorkee, 2001), p. 245
6. M. K. Weulersse, G. Moulin, G. P. Billard, and G. Pierotti, *Materials Science Forum* **461–464**, 973 (2004).
7. M. M. Barbooti, S. H. Al-Madfai, and J. Nassouri, *Thermochimica Acta* **126**, 43 (1988).
8. S. Kamal, R. Jayaganthan, S. Prakash, and S. Kumar, *Journal of Alloys and Compounds* **463**, 358 (2008).
9. I. Gurrappa and A. S. Rao, *Surface & Coatings Technology* **201**, 3016 (2006).
10. B. S. Sidhu and S. Prakash, *Wear* **260**, 1035 (2006).
11. N. Eliaz, G. Shemesh, and R. M. Latanision, *Engineering Failure Analysis* **9**, 31 (2002).
12. B. Q. Wang and S. W. Lee, *Wear* **203–204**, 580 (1997).
13. B. Wang and S. W. Lee, *Wear* **239**, 83 (2000).
14. B. Q. Wang, *Wear* **199**, 268 (1996).
15. B. Q. Wang and Z. R. Shui, *Wear* **253**, 550 (2002).
16. M. H. Guo, Q. M. Wang, P. L. Ke, J. Gong, C. Sun, R. F. Huang, and L. S. Wen, *Surface & Coatings Technology* **200**, 3942 (2006).
17. G. W. Goward, *Surface & Coatings Technology* **108–109**, 73 (1998).
18. T. N. Rhys-Jones and N. Swindells, *Corrosion Science* **25**, 559 (1985).
19. H. S. Sidhu, B. S. Singh, and S. Prakash, *Surface & Coatings Technology* **202**, 232 (2007).
20. N. Bala, H. Singh, and S. Prakash, *Journal of Thermal Spray Technology* **19**, 110 (2010).

21. A. Ul-Hamid, *Materials Chemistry and Physics* **80**, 135 (2003).
22. B. S. Sidhu and S. Prakash, *Surface & Coatings Technology* **166**, 89 (2003).
23. H. Singh, D. Puri, and S. Prakash, *Surface & Coatings Technology* **192**, 27 (2005).
24. G. Sundararajan, *Wear* **145**, 251 (1991).
25. G. Sundararajan, *Wear* **162–164**, 773 (1993).
26. T. Sundararajan, S. Kuroda, and F. Abe, *Metallurgical and Materials Transactions A* **36A**, 2165 (2005).
27. T. Sundararajan, S. Kuroda, T. Itagaki, and F. Abe, *ISIJ International* **43**, 95 (2003).
28. T. Sundararajan, S. Kuroda, and F. Abe, *Corrosion Science* **47**, 1129 (2005).
29. G. A. Kolta, L. F. Hewaidy, and N. S. Felix, *Thermochimica Acta* **4**, 151 (1972).
30. M. Seierdten and P. Kofstad, *High Temperature Technologies* **5**, 115 (1987).
31. J. Swaminathan, S. Raghavan, and S. R. Iyer, *Transactions of the Indian Institute of Metals* **46**, 175 (1993).
32. G. C. Fryburg, F. J. Kohl, C. A. Stearns, and W. L. Fielder, *Journal of the Electrochemical Society* **129**, 571 (1982).
33. M. H. Guo, Q. M. Wang, P. L. Ke, J. Gong, C. Sun, R. F. Huang, and L. S. Wen, *Surface & Coatings Technology* **200**, 3942 (2006).
34. M. H. Guo, Q. M. Wang, P. L. Ke, J. Gong, C. Sun, R. F. Huang, and L. S. Wen, *Corrosion Science* **48**, 2750 (2006).
35. T. S. Sidhu, R. D. Agarwal, and S. Prakash, *Materials Science and Engineering A* **430**, 64 (2006).
36. T. S. Sidhu, R. D. Agarwal, and S. Prakash, *Surface & Coatings Technology* **201**, 1602 (2006).
37. T. S. Sidhu, R. D. Agarwal, and S. Prakash, *Scripta Materialia* **55**, 179 (2006).
38. H. Singh, D. Puri, and S. Prakash, High Temperature Oxidation Behaviour of Plasma Sprayed NiCrAlY Coatings on Ni-based Superalloys in Air, in *Proceedings of the International Symposium of Research Students on Material Science and Engineering (ISRS)*, December 20–22 (Department of Metallurgical and Materials Engineering, Indian Institute of Technology Madras, Chennai, 2004), p. 1.
39. S.N. Tiwari and S. Prakash, Hot Corrosion Behaviour of an Iron-Base Superalloy in Salt Environment at Elevated Temperatures, in *Proceedings of the Symposium Metals and Materials Research*, 4–5th July (Indian Institute of Technology Madras, Madras, 1996), p. 107.
40. S.N. Tiwari and S. Prakash, Studies on the Hot Corrosion Behaviour of Some Superalloys in Na_2SO_4–V_2O_5, in *Proceedings of the SOLCEC*, 22–24th January (Kalpakkam, 1997), Paper C33.
41. S. N. Tiwari and S. Prakash, *Materials Science and Technology* **14**, 467 (1998).
42. V. Chawla, A. Chawla, B. S. Sidhu, S. Prakash, and D. Puri, *Journal of Minerals and Materials Characterization and Engineering* **10**, 583 (2011).
43. V. Chawla, A. Chawla, B. S. Sidhu, S. Prakash, and D. Puri, *Journal of Minerals and Materials Characterization and Engineering* **9**, 1037 (2010).
44. V. Chawla, D. Puri, S. Prakash, A. Chawla, and B. S. Sidhu, *Journal of Minerals and Materials Characterization and Engineering* **8**, 715 (2009).
45. V. Chawla, S. Prakash, D. Puri, and B. Singh, *Journal Australian Ceramic Society* **44**, 56 (2008).
46. H. Singh, S. Prakash, and D. Puri, *Materials Science and Engineering A* **444**, 242 (2007).
47. B. Singh, *Studies on the Role of Coatings in Improving Resistance to Hot Corrosion and Degradation*. Ph.D. Thesis, IITR, Roorkee, India (2003).
48. N. Bala, H. Singh, and S. Prakash, *Mater Design* **31**, 244 (2010).
49. L. Shi, *Oxidation of Metals* **40**, 197 (1993).
50. S. E. Sadique, A. H. Mollah, M. S. Islam, M. M. Ali, M. H. H. Megat, and S. Basri, *Oxidation of Metals* **54**, 385 (2000).
51. K. Sachs, *Metallurgia* **Apr**, 167 (1958).
52. D. Das, R. Balasubramaniam, and M. N. Mungole, *Journal Materials Science* **37**, 1135 (2002).
53. M. Schutze, M. Malessa, V. Rohr, and T. Weber, *Surface & Coatings Technology* **201**, 3872 (2006).
54. S. Roure, F. Czerwinski, and A. Petric, *Oxidation of Metals* **42**, 75 (1994).
55. M.S. Li, *High Temperature Corrosion of Metals* (The Industry of Metallurgy Publisher, 2001).
56. J. A. Goebel, F. S. Pettit, and G. W. Goward, *Metallurgical Transactions* **4**, 261 (1973).
57. R. A. Rapp and Y. S. Zhang, *JOM Journal of the Minerals Metals and Materials Society* **46**, 47 (1994).
58. A. H. Dent, A. J. Horlock, D. G. McCartney, and S. J. Harris, *Journal of Thermal Spray Technology* **8**, 399 (1999).

59. F. H. Stott, Principles of growth and adhesion of oxide scales. in *The role of active elements in the oxidation behaviour of high temperature metals and alloys*, ed. E. Lang (Elsevier Applied Science, London, 1998).
60. L. Li, R. Zhu and F. Gesmundo, *Journal of Materials Science and Technology* **12**, 445 (1996).
61. T. Sundararajan, S. Kuroda, and F. Abe, *ISIJ International* **44**, 139 (2004).